ELSEVIER

Contents lists available at ScienceDirect

Chemical Engineering Journal

journal homepage: www.elsevier.com/locate/cej



Hollow fiber membrane supported metal organic framework-based packed bed for gas/vapor adsorption



Yufeng Song, Kamalesh K. Sirkar

Otto York Department of Chemical and Materials Engineering New Jersey Institute of Technology University Heights Newark, NJ 07102 USA

ARTICLE INFO

Keywords:
Metal-organic framework
Hollow fiber membrane support
Gas adsorption
Ammonia removal
Porous Nylon membrane
Nanocrystals and microcrystals

ABSTRACT

Crystalline metal-organic frameworks (MOFs) with high porosity have high sorption capacities for various gases. Their fragile and pulverulent characteristics have prompted significant efforts to prepare shaped bodies e.g., pellets, granules for use in adsorbers. A hollow fiber membrane-based strategy is adopted since hollow fiber membrane (HFM) modules are highly preferred for industrial separation processes due to very high surface area provided per unit device volume and their easy scalability. We report herein a solvothermal synthesis method whereby nanocrystals of the MOF, UiO-66-NH2, are synthesized directly inside submicron pores of hydrophilic hollow fiber membranes of Nylon 6 as well as in the bores of the HFMs. Nanocrystals of around 100 nm populate HFM pores. Cylindrical modules containing such HFMs and MOF nanocrystals and microcrystals in membrane pores, HFM bores and the extra capillary space were studied for adsorption of ammonia from a dilute gas stream. High values of ammonia breakthrough time were achieved. The corresponding behaviors of three MOF configurations namely, MOF in membrane pores, MOF in membrane pores and the HFM bores and MOF present in membrane pores, HFM bores and in extra capillary space were studied. The values of time/MOF weight achieved were very high. The MOFs synthesized were characterized by Scanning electron microscopy (SEM), Fouriertransform infrared spectroscopy (FTIR), powder X-ray diffractometer (PXRD), Brunauer-Emmett-Teller (BET) adsorption isotherms, surface area, and pore size distribution. High performance of HFM-supported MOF-based scalable devices for gas/vapor adsorption has been demonstrated with values of 20,000 min/g of MOF for trace ammonia breakthrough from humid ammonia feed gas stream employed. Other potential uses of such devices for adsorbing 2 to 3 gases and liquid phase adsorption have also been discussed.

1. Introduction

For adsorption-based separations, membrane separations, gas storage applications, catalytic degradations/reactions, barriers for ions in solution, barriers or masks for toxic gases and vapors, metal–organic framework (MOF) materials are of great interest [1–14] There are quite a few studies where MOFs were used in mixed matrix polymeric membranes where MOFs are dispersed in a polymer matrix for membrane gas separation [2]. There are others where a MOF based membrane was prepared for membrane gas separation [9,11]. For example, pure ZIF-8 MOF based membrane was formed on the internal surface of porous polymeric hollow fibers of polyamide-imide for propylene separation [11]. Here we focus on adsorption of a gas/vapor from a gaseous medium by MOFs.

Selective adsorption/desorption of gases and vapors from gas streams/air is practiced extensively in large-scale industrial applications as well as for cleaning up air streams having toxic gases and vapors. Novel sorbent materials such as MOFs, material structures and sorption methods continue to be developed for such applications as well as for protection against exposures to toxic gases and vapors encountered during industrial accidents [15]. The latter include ammonia, chlorine, sulfur dioxide, hydrogen sulfide, hydrogen cyanide, cyanogen chloride etc. [16]. In addition, CO₂ sorption/recovery by MOFs is also of interest. The MOF studied here is UiO-66-NH₂.

MOF crystals are intrinsically fragile. Therefore, their applications utilize structures or configurations that overcome such limitations and yet allow access to their high porosity for selective sorption/storage and metallic links for catalytic destruction/selective sorption activities. Such structures are in general not able to remove toxic gases and vapors completely on a steady-state basis so that time-dependent adsorption-based processes are needed. We are focusing here on MOF-containing structures/formats that allow adsorption-based gas separation/toxic

E-mail address: sirkar@njit.edu (K.K. Sirkar).

^{*} Corresponding author.

gas removal at various scales of operation. Removal of the toxic gas, NH_3 , is being considered.

Earlier studies [16-18] focused on MOF sorption properties via for example packed beds of MOF, UiO-66-NH₂, in the form of 20 \times 40 mesh size granules. Other structures studied include: MOF-functionalized nonwoven fiber mats enabled by atomic layer deposition [19-20]; ink of polyvinylidene fluoride (PVDF) containing dispersed micron-sized MOF particles forming a thin film for use in a membrane reactor [21]. Shaping of the MOF particles into appropriate size is important for use in various packed-bed applications; the size considered reasonable is 10 \times 20 mesh. The pulverulent tendency of MOFs has posed major problem in terms of shaping needed to achieve the ultimate commercially usable form; the shapes explored include pellets, monoliths, granules etc. [22]. The NH₃-air purification performances of UiO-66-COOH in bead, tablet and extrudate forms were compared to those of commercial carbonbased materials (type K adsorbents from 3M and Norit) and found to be superior especially under dry conditions [23]. It has been suggested that a mechanically weak pellet is obtained by pressing a MOF powder into pellets; however, the mechanical stability of the pellet is increased enormously by a Matrimid membrane coating on the pellet without affecting sorption capacity by much [24].

As pointed out by Younas et al. [25], although high structural porosity is an inherently attractive property of MOFs for various chemical separations and other applications, highly porous MOFs are mechanically unstable; when mechanically loaded, the pore structure can collapse and there may be even phase change. Further, MOFs as synthesized are obtained as loose powders and need consolidation. Nandasiri et al. [26] pointed out that shaping and densification of MOFs via mechanical compression, palletization, extrusion etc. can distort the pore structure in particular MOFs and can lead to as much as 50 % loss of BET surface area measured. Khabjina et al. [23] report the following values of BET N₂ surface area (m²/g) and micropore volume (cm³/g) for the following densified MOFs for UiO-66-COOH: compressed pellets, 614, 0.24; extrudates, 418, 0.15; beads, 359, 0.12; the corresponding values for the original powder are,710, 0.28. Shah et al. [27] dealt

extensively with the mechanical properties of shaped MOFs and identified the many engineering challenges of using MOFs in various applications. It has also been pointed out that UiO-66 type MOFs have lower porosity and are mechanically more stable [25].

We report here a different structure/configuration for handling nanocrystals and microcrystals of the MOF, UiO-66-NH₂. The MOF UiO-66-NH₂ was selected because it shows high stability over a pH range of 0–12, high thermal stability, stability toward oxidative environments, moisture and steam [25]. It is considerably due to its Zr (IV) based structure. We employ porous hollow fiber membrane (HFM)-based cylindrical modules where conceptually the HFMs are relatively close to one another (in industrial membrane gas separation, HFMs are highly packed in a module). Therefore, a few MOF microcrystals are located in the extra fiber space just as a few microcrystals are located in the bore of the HFMs at any location. Fig. 1 illustrates the basic configuration.

The microcrystals in the HFM bore and the extra capillary space do get support from the HFM wall by friction and are unlikely to be subjected to the load of MOF microcrystals present above in a vertical module. This issue does not arise if the HFM module is used horizontally. Hollow fiber membranes are used during MOF synthesis such that the pores were loaded with the MOF synthesis solution and end up with nanocrystals in the submicron size HFM pores; the bores of HFMs are also populated with microcrystals and nanocrystals during MOF synthesis. The porous HFMs of interest are of hydrophilic Nylon 6, 6; HFMs of other polymers and wetting properties can be utilized as well.

Since we employ dimethyl formamide (DMF)-methanol based solution for MOF synthesis, Nylon membrane pores are spontaneously wetted by the solution to be used for solvothermal synthesis of MOF. This is unlike the use of flat ePTFE membranes used earlier [28] where an extensive and multistep solvent exchange process had to be undertaken. It started with pure methanol as solvent (which wets ePTFE pores easily) in the first step of a solvent exchange process which ultimately ended with 80 % DMF-20 % methanol solution of the reactants in the pores of flat ePTFE membrane which is not spontaneously wetted by the polar aprotic solvent DMF. The present Nylon membrane-based process

Hollow Fiber Membrane Module Based Adsorbent Bed

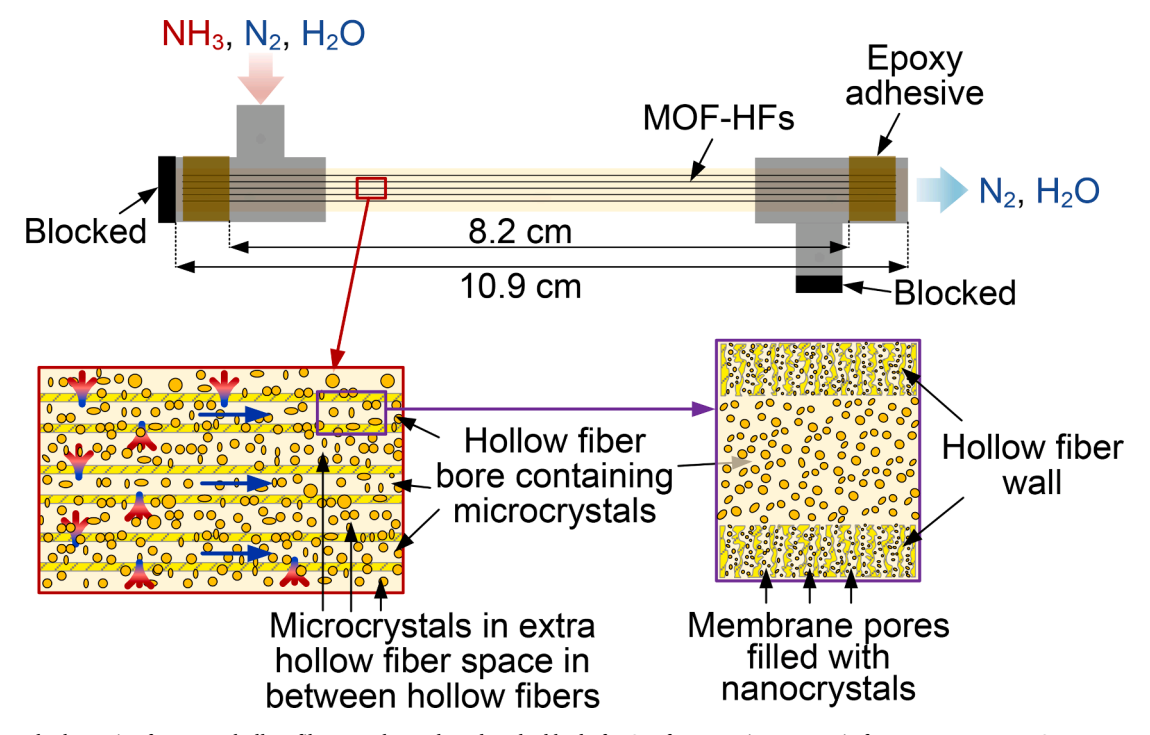


Fig. 1. Conceptual schematic of a porous hollow fiber membrane-based packed bed of MOFs for removing ammonia from a gas stream: MOFs present as nanocrystals in submicron pores of HFM wall and as microcrystals in HFM bore and the extra capillary space.

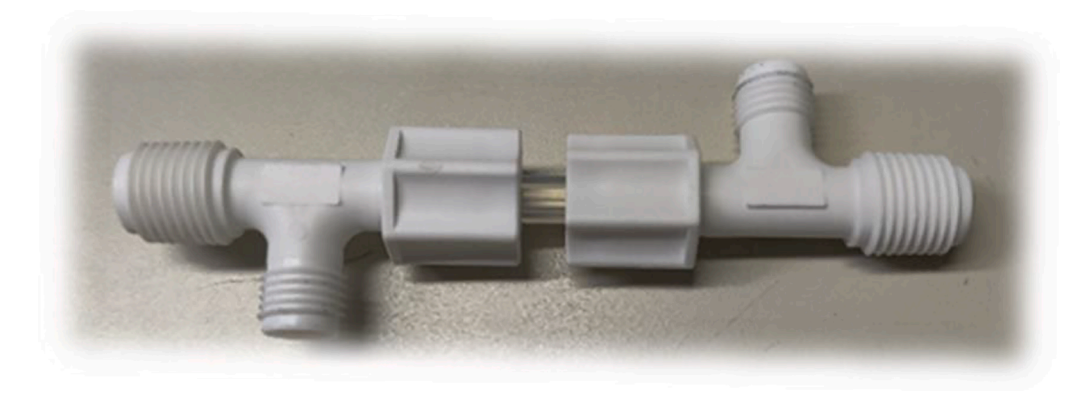


Fig. 2. Photo of the hollow fiber membrane module with hollow fiber membranes visible through the transparent shell in the center.

is simpler than the recent one where vacuum facilitated introduction of the DMF-methanol solution was undertaken with a flat ePTFE membrane [29]. The current approach of using hydrophilic porous Nylon HFM may also be used with hydrothermal MOF synthesis [23]. Our strategy here is distinct from that used to make highly porous MOF-containing flat membranes for liquid separations by a thermally induced phase separation-hot pressing strategy using MOFs, polyethylene and paraffin which is extracted out later [30].

There are other reasons for selecting Nylon hollow fiber membranes. Nylon is a highly inert polymer when it comes to organic solvent resistance. Further, its melting point is very high; for Nylon 6 employed here, it is around 268 $^{\circ}$ C. That is why it was selected for this application where the MOF synthesis temperature is not very low. It also has a high tensile strength.

The module type shown schematically in Fig. 1 (Fig. 2 has a photo) was used to study breakthrough of NH₃ from a N₂ stream under the following three module configurations: Type I-HFMs containing nanocrystals in the membrane pores only; Type II-HFMs having nanocrystals in the membrane pores and microcrystals in the HFM bore; Type III-HFMs having nanocrystals in the membrane pores, microcrystals in the HFM bore and in the shell-side inter-fiber space. The MOFs in various locations have been characterized. Successful regeneration of the MOF adsorbents has also been investigated.

2. Materials and methods

2.1. Materials and chemicals

Nylon 6 (polyamide PA6) HFMs (hydrophilic; pore size: $0.2~\mu m$, porosity: 75~%, OD: $1,000~\mu m$; ID: $600~\mu m$; Enka America Inc., Asheville, NC) were used. The HFM properties and HFM module details are provided in Tables 1 and 2 respectively. Expanded polytetrafluoroethylene (ePTFE) membrane (GMM-404: pore size, $0.45~\mu m$; porosity, 80~%; thickness, $79~\mu m$; W.L. Gore, Elkton, MD) was used for filtration. Methanol (EMD Millipore, $\geq 99.8~\%$), DMF (Fisher Chemical, 99.9~%), zirconium (IV) chloride (Alfa AesarTM, >99.5~%), 2-aminoterephthalic acid ($H_2BDC-NH_2$, Acros OrganicsTM, 99~%) were used for UiO-66-NH₂ MOF synthesis.

Table 1 Physical properties* of hollow fiber membranes used.

Hollow-Fiber Membrane	Material	Pore Size µm	OD μm	ID μm	Porosity	Bubble Point** bar
Nylon 6 (hydrophilic)	Polyamide 6	0.2	1,000	600	0.75	3.7

^{*} From manufacturer's information.

Table 2
Details of hollow fiber membrane modules.

Membranes	Nylon-6			
Shell	Teflon® FEP semi-clear tubing, 1/8" ID*, 1/4" OD**			
Number of hollow fibers	5			
Active length (cm)	8.2			
Shell-side void volume fraction	0.50			
Surface area for each hollow fiber (cm ²)	Based on ID* 1.418			
	Based on OD** 2.576			

^{*}Inside diameter; ** Outside diameter.

2.2. MOF synthesis in Nylon 6 HFMs and preparation of MOF-loaded Nylon HFM-based modules

This synthesis may be carried out in two ways. Using loose hollow fiber membranes, one can carry out MOF synthesis under appropriate solvothermal/hydrothermal synthesis conditions. Alternately, one can take a hollow fiber membrane module with hollow fibers potted into a tube-sheet at both ends, fill the internal volume in the module with the synthesis solution and carry out the synthesis. The procedure employed with the first approach is described here. All membrane modules used were built with such loose HFMs which underwent the solvothermal synthesis in a demanding solvent environment.

Loose Nylon hollow fiber membranes were inserted, wetted and submerged in mixed reactant-containing solution placed in a Teflonlined pressure vessel. The solution was prepared by dissolving 70 mmol NH2-H2BDC in 140 g DMF and mixing it with 70 mmol ZrCl4 dissolved in 35 g methanol along with 5 mmol/L of sodium dodecyl sulfate (SDS). Then it was sonicated for 15 min by an ultrasonic processor (Cole Parmer, Vernon Hills, IL). Before closing the lid of the vessel, the vessel was purged with high purity N_2 to remove air. The vessel was put into oven at 120 °C for 18 hr. After the treatment, the HFMs were washed with methanol. For the MOF-filled HFMs used in module Type I, methanol was pushed into the tube side of the hollow fibers to remove the MOF crystals synthesized in the bore of the HFMs. For the MOF-filled HFMs used in module Type II, the hollow fibers were rinsed with methanol to clean the outside of the MOF-filled HF without pushing methanol into the tube side to remove MOF crystals from the HFM bore. The MOF-filled Nylon HFMs were next dried at 60 $^{\circ}\text{C}$ for 2 weeks in a vacuum drying oven (Zenith Lab Inc., Brea, CA) under a vacuum of 18 in Hg. We have not optimized the duration of the drying procedure; the extended time used was to ensure that drying was complete. In other studies [28,29] using this MOF under identical synthesis conditions using flat microporous ePTFE membranes, drying carried out at 50 °C for 4 days under vacuum was found to be sufficient. After sealing the MOF-HFMs into the module (procedure described below),

^{**} Against water.

the MOF-HFM module was kept in a desiccator connected to fume hood vacuum (18 in Hg) at 50 $^{\circ}$ C for 10 days.

To prepare the MOF-filled Nylon hollow fiber membrane module (shown in Fig. 1), five MOF-filled HFMs were potted in the module shell (Teflon® FEP semi-clear tubing, 1/8'' ID, 1/4'' OD) by epoxy adhesive (Loctite EA M=21HP TM). The total length of each HFM in the module is 10.9 cm. Around 1.35 cm length of the hollow fibers at each end were potted with an epoxy adhesive. The active length of the hollow fiber is 8.2 cm (Fig. 2). For each hollow fiber, the surface areas based on virgin Nylon HF ID and OD are: outer surface area: 3.142 mm \times 8.2 cm = 2.576 cm 2 ; inner surface area: 1.729 mm \times 8.2 cm = 1.418 cm 2 . For 5 HFMs in the module, the total outer surface area is 12.88 cm 2 for a total inner surface area of 7.09 cm 2 .

For preparation of the Type III MOF-HFM module where MOFs are located in hollow fiber membrane pores, the HFM bores and the extra capillary space, 5 g of the UiO-66-NH2 MOF, obtained during the preparation of Type I and Type II MOF-filled HFMs, were added into 100 ml methanol to prepare a MOF suspension. Magnetic stirrer was used to prepare the MOF suspension and maintain the stability of the suspension. The MOF microcrystals and nanocrystals were introduced into the shell side of the Type II MOF-HFM module by pushing the MOF suspension into the module by N₂ gas (pressure 1–2 psig) and blocking the expulsion of MOF microparticles and nanoparticles by a GMM 404 ePTFE membrane (pore size: 0.45 μm) and cotton sliver. Figs S1 and S2 show respectively the schematic and photo of the setup for introducing MOF nanocrystals into shell side of the MOF-HFM module. The module was dried at 50 °C under vacuum for 3 days. The weight increase due to MOF nanocrystals filled in the shell side was 0.2 g. MOF loading % in the shell side was \sim 50 %. Then, one end of the tube side was sealed by epoxy as shown in Fig. 1. Fig. S3 shows the photos of the completed Type III MOF-HFM module.

2.3. Characterization of MOF-filled Nylon 6 hollow fiber membrane

Empyrean multipurpose powder X-ray diffractometer (PXRD) with PIXcel 1D detector (Serial 202627, PANalytical) was used to obtain the powder X-ray diffraction patterns of virgin Nylon 6 HFM and MOF-filled HFM. PXRD patterns of all samples were scanned by Cu K(alpha) radiation ($\lambda=1.54$ Å, 40 mA, 45 kV) from 5° to 60° of 2θ , step size $=0.0260^\circ$ (2θ), scan step time =99.176 s. Fourier-transform infrared spectroscopy (FTIR) was carried out in an Agilent Cary 670 FTIR spectrometer for FTIR spectra of samples. 32 scans were taken per sample over 6000-400 cm $^{-1}$ with a resolution of 4 cm $^{-1}$.

Scanning electron microscopy (SEM) was implemented using a separate field emission-scanning electron microscope (FE-SEM, Model LEO1530vp) to obtain the membrane cross sectional images. The samples were mounted on the SEM stubs by carbon tape and coated with 10 nm of gold by Turbomolecular pumped coater (Model EMS Q150T ES).

Optical microscopic photos of the cross-sectional area/bore of a single hollow fiber membrane were obtained by a Raman Imaging Microscope (DXR2xi, Thermo Scientific).

 $\rm N_2$ isotherm curves of samples were collected by an automated gas sorption analyzer (Model #: ASIQM000000-6, Quantachrome Instruments, Boynton Beach, FL). Pore size distribution and Brunauer-Emmett-Teller (BET) surface area were calculated by commercial DFT software combined with the instrument operation interface. Before starting BET measurement, membrane samples were degassed at 70 $^{\circ}\mathrm{C}$ for 48 hr and UiO-66-NH $_2$ MOF samples were degassed at 120 $^{\circ}\mathrm{C}$ for 18 hr.

The tensile strengths of virgin Nylon hollow fiber membranes and the Nylon hollow fiber membranes which underwent the MOF synthesis in the reactor were measured at room temperature in an Instron Model 3342 Testing System (Instron, Norwood, MA). The hollow fiber membrane cross sectional area was $0.548~{\rm mm}^2$. The stretching rate was $20~{\rm mm/min}$.

2.4. Ammonia breakthrough experiment

The dead-end set up for the breakthrough testing using ammoniasensing chips in the flow-through mode is shown in Fig. S4. A stream of 200 ppmv ammonia in N_2 calibration gas (Gasco, Oldsmar, FL) was mixed with wet (relative humidity, RH $=\sim95~\%)~N_2$ gas before introduction of the mixed gases into the membrane module. The flow rates of these two streams were adjusted to 5 cm³/min respectively by two mass flow rate controllers (Model 8272–0453 and 829-C4212T, Matheson—Trigas, Montgomeryville, PA). The ammonia concentration at module outlet was obtained by a CMS analyzer (Draeger, Telford, PA) with ammonia CMS chips (0.2 – 5 ppm, Model 6406550, 2 – 50 ppm, Model 6406130, 10 – 150 ppm, Model 6406020, Draeger, Telford, PA).

2.4.1. Freshly made MOF-filled Nylon HFs module

The freshly made MOF-filled Nylon HFs were next dried at 60 $^{\circ}$ C for 2 weeks in a vacuum drying oven (Zenith Brea, CA). After potting MOF-HFs into a module, the freshly made MOF HF-based module was kept in a desiccator connected to the lab hood vacuum at 50 $^{\circ}$ C for 10 days.

2.4.2. Regeneration of MOF-filled Nylon HFs module

The MOF-filled HFs in the module used in the ammonia breakthrough testing described earlier with 100 ppmv wet ammonia calibration gases were regenerated by heating in a vacuum drying oven (Zenith Lab Inc., Brea, CA) at 60 $^{\circ}$ C for 4 days and heating in a desiccator (connected to hood vacuum) at 50 $^{\circ}$ C for 4 days. Then, the blocking performances of the regenerated MOF-filled HFs module to ammonia were measured by the same steps as above.

3. Results and discussion

3.1. Porous Nylon HFMs and MOF nanocrystals in submicrometer HFM pores

Modules of HFMs can provide very high surface area/device volume going up to 35–40 cm²/cm³. Correspondingly, these structures can also create a very large reservoir of adsorbent surface area per unit device volume. Fig. 3 shows the scanning electron micrograph (SEM) based cut section of a single HFM and multiple Nylon HFMs with each HFM outside diameter (OD)/inside diameter (ID) being $1000/600 \mu m$ (Table 1). The surface area/device volume obtained in a module of hollow fiber membranes of diameter d and hollow fiber packing fraction in the shell of ϵ is (4/d) ϵ . The smaller the hollow fiber membrane diameter, the higher is the surface area of the hollow fiber membranes/ device volume. Since the ID of the hollow fibers here is $600 \mu m$, the corresponding value of membrane surface area/device volume for a hollow fiber packing fraction of 0.4 is 26.67 cm²/cm³. Hollow fiber membrane diameters in industrial/commercial use vary from 200 to 1000 μm +. The smallest hollow fibers can pack a very high surface area/device volume.

Fig. 4a shows a 30,000x magnification-based SEM of the cross-sectional details of any location in the porous wall of a single Nylon HFM filled with nanocrystals of the MOF synthesized in situ. Virtually all MOF crystals dispersed throughout the porous wall are around 100 nm. Fig. 4b taken at a lower magnification (10,000x) reinforces such a narrative. It is also clear that there is still a large void volume available inside the porous HFM wall cross section so that there is unlikely to be significant gas flow pressure drop. Given such an excess unoccupied space in the pores in the membrane wall, one could undertake potentially another round of hydrothermal synthesis of MOFs to increase the loading of MOF nanocrystals in the membrane pores [28,29] the hollow fiber membrane wall porosity being 0.75 (Table 1). Fig. 4c shows a collection of microcrystals appearing as an object with a very rough surface inside the internal diameter of the hollow fiber membrane whose boundary is visible in the background shadow in the middle photo.

Solution phase synthesis of this MOF does not produce high enough

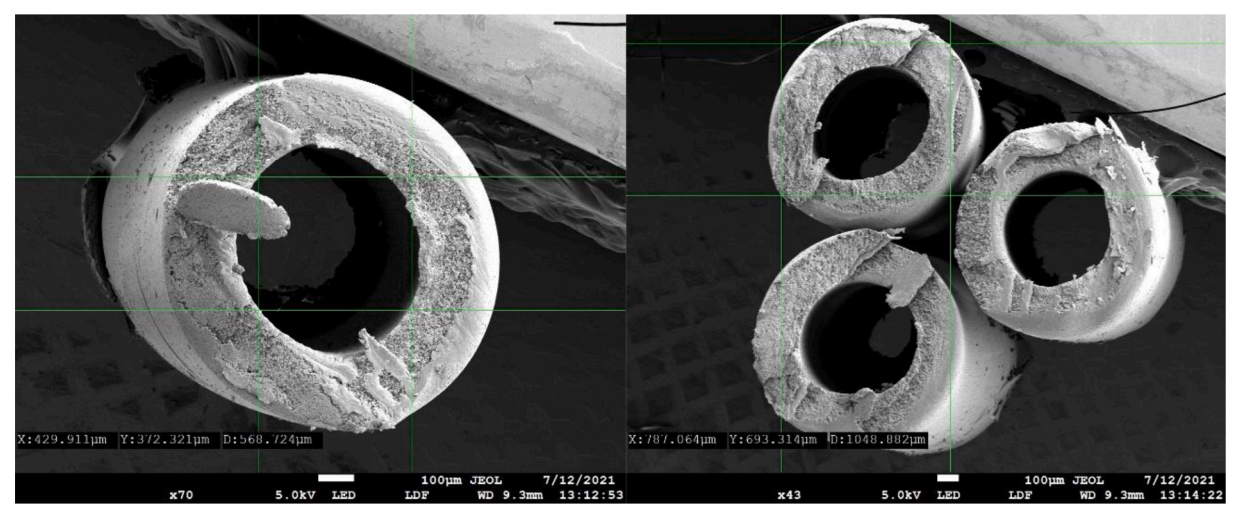


Fig. 3. SEMs of cross section of one Nylon HFM (left) and cross sections of three contiguous Nylon HFMs (right).

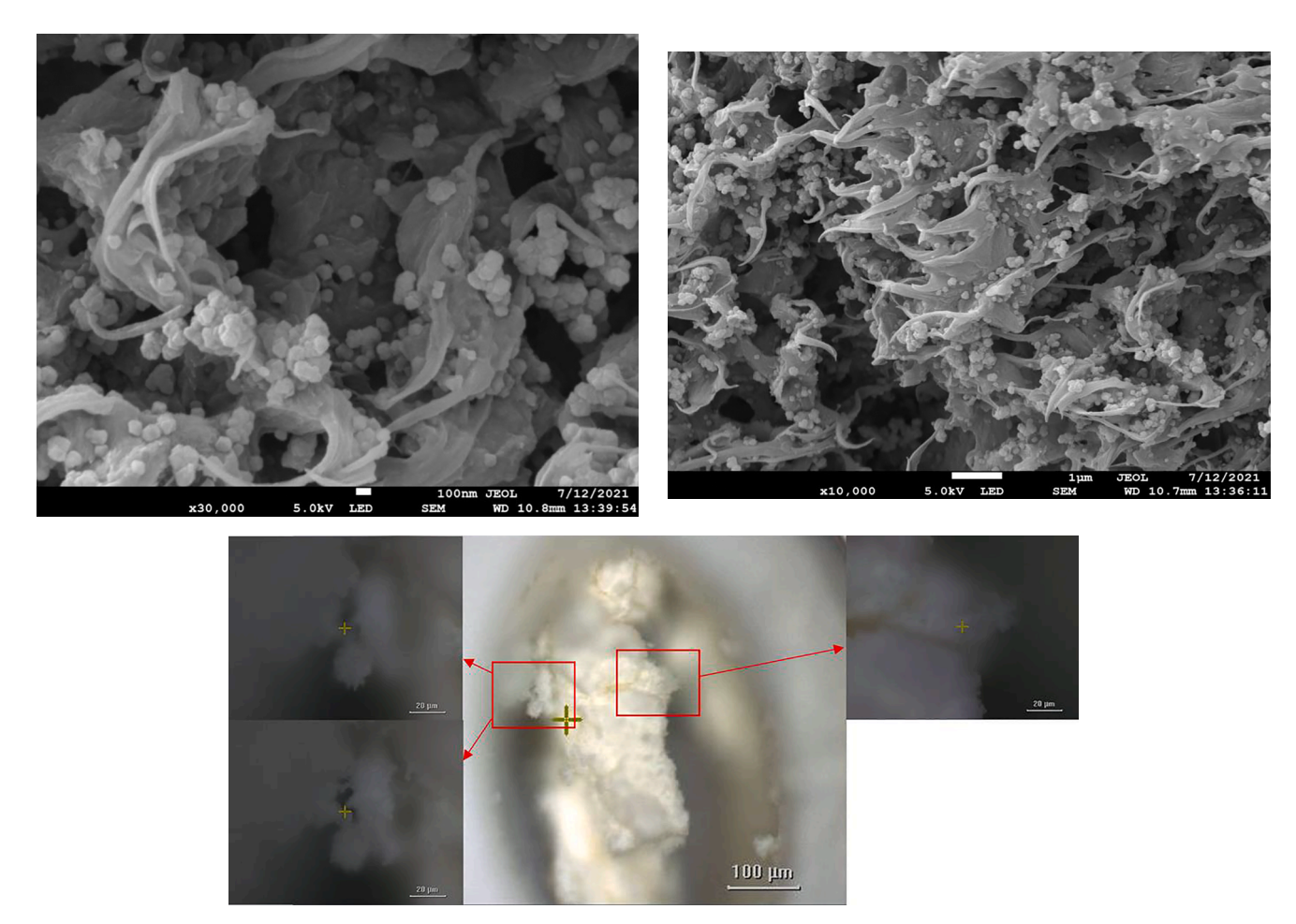
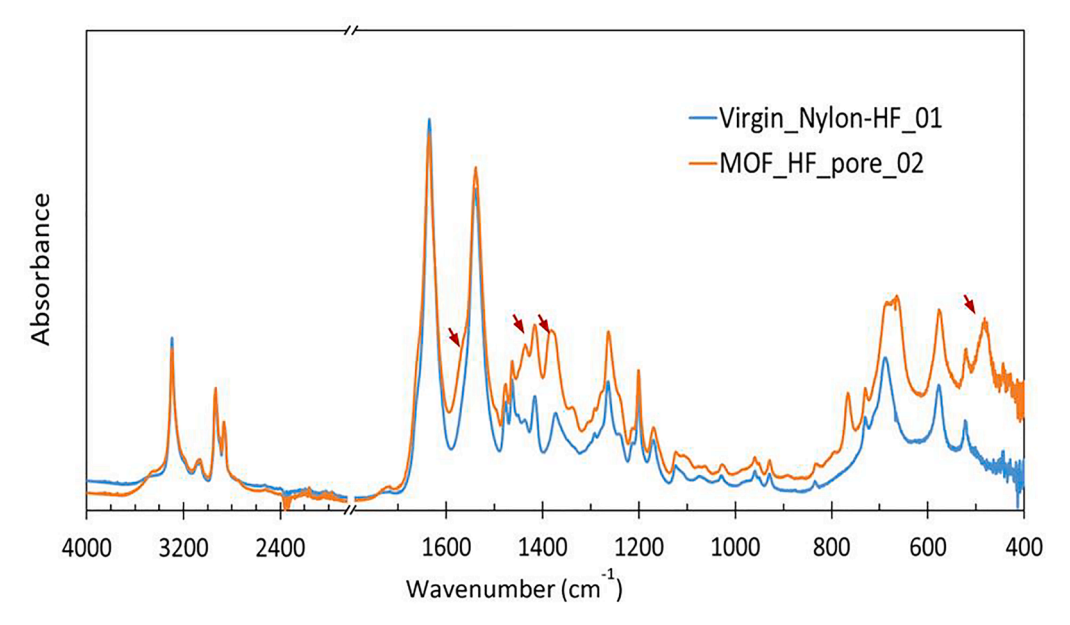


Fig. 4. (a), 4(b). Two SEM images of the cross section of a part of the porous wall of MOF-filled Nylon hollow fiber membrane at varying magnifications: (a) x30,000 (top, left) and (b) x10,000 (top, right). Fig. 4(c). Optical microscope photos of the MOF crystals in the bore of a hollow fiber membrane taken by a Raman Imaging Microscope (bottom figure).

crystal density for clogging the regions filled with the solution. This is just as valid for the extra capillary space in between the hollow fibers and the hollow fiber bore as for the region of membrane pores. In fact, as mentioned above, one can carry out additional synthesis steps to develop a higher crystal density as was done in [28,29] in the pores of flat membranes. Gas phase pressure drop from the module inlet to outlet is also an indicator of clogging on the shell side and the tube side. We did

not encounter much pressure drop. The same is valid for liquid phase adsorption in such a configuration.

Fig. 5 illustrates the FTIR spectra of the virgin Nylon HFM as well as those of the UiO-66-NH $_2$ MOF-filled Nylon HFM. In our previous study [28], the two bands between 1566 cm $^{-1}$ and 1400 cm $^{-1}$ and the peaks at 659 cm $^{-1}$ and 477 cm $^{-1}$ indicated the carboxylate and Zr–(OC) bond of UiO-66-NH $_2$ MOF. Since the Nylon membrane also has some absorption



 $\textbf{Fig. 5.} \ \ \textbf{FTIR} \ \ \textbf{spectra of UiO-66-NH} \ \ \textbf{MOF-filled Nylon hollow fiber membrane} \ \ \textbf{and virgin Nylon hollow fiber membrane}.$

in these band ranges, some peaks of MOF are masked by the absorption of the Nylon membrane. Some differences are still clearly displayed, such as the peaks close to $1400~{\rm cm}^{-1}$ and $477~{\rm cm}^{-1}$, which are marked by red arrows. These spectra demonstrate that this MOF could be successfully synthesized using equimolar amounts of $\rm ZrCl_4$ and $\rm H_2BDC\text{-}NH_2$ in 80 % DMF- 20 % methanol in the Nylon HFM pores.

3.2. Ammonia adsorption behavior of the HFM-based packed bed

Ammonia adsorption properties of such MOF nanocrystal loaded HFM pores are shown in Fig. 6a and 6b. This behavior was investigated by introducing 100 ppmv (70.8 mg/m³) NH₃-containing gas stream (relative humidity (RH), 50 %) flowing at 10 cm³/min into the shell-side

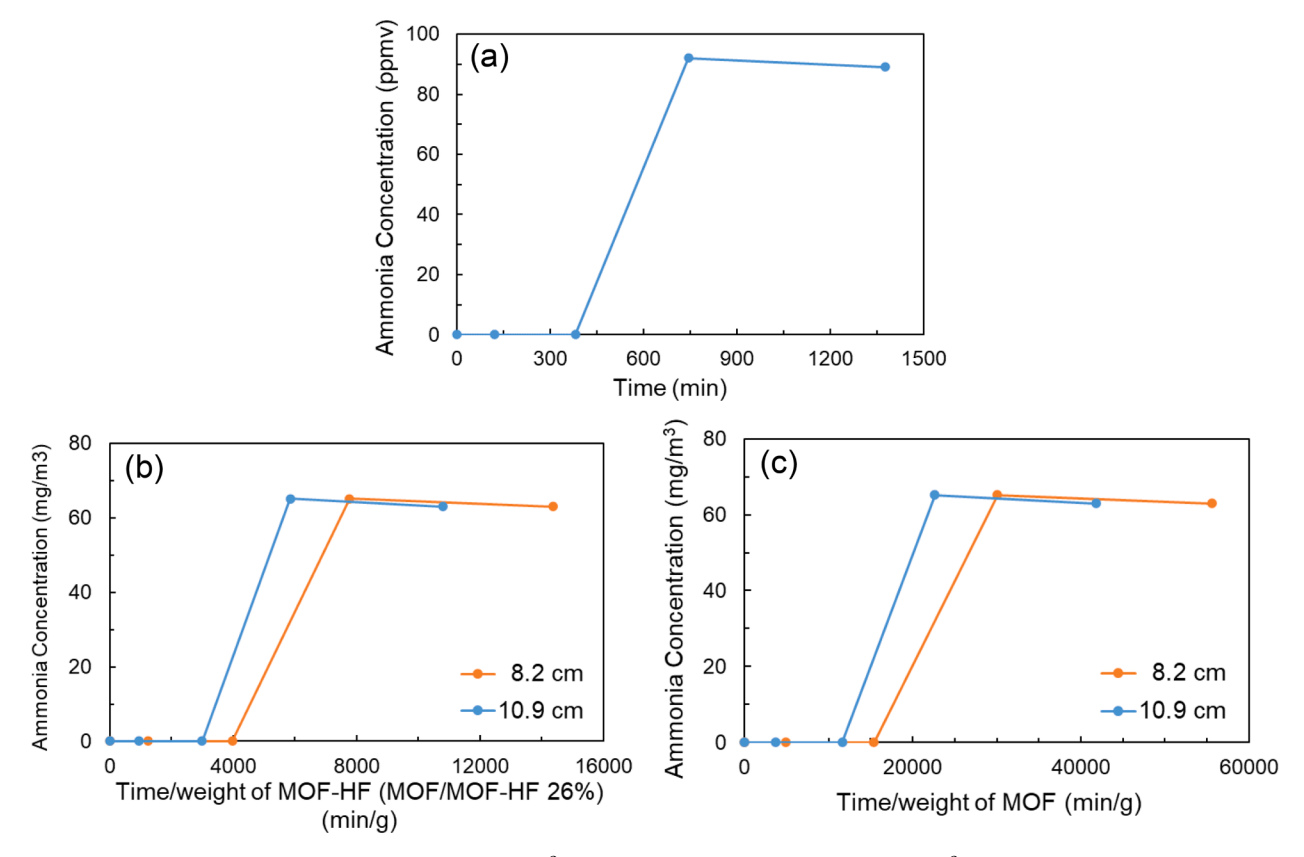


Fig. 6. (a) Ammonia breakthrough data with 100 ppmv (70.8 mg/m 3) NH $_3$ -containing gas stream flowing at 10 cm 3 /min at a RH of \sim 50 % through UiO-66-NH $_2$ MOF-loaded Nylon hollow fiber membrane module (MOF loaded in the HFM pores only); (b) breakthrough data normalized by weight of MOF-HFMs; (c) breakthrough data normalized by weight of MOF only. Blue lines plot the data calculated based on the whole length (10.9 cm) of the HFMs; orange lines plot the data calculated based on the active length (8.2 cm) of the HFMs. (For interpretation of the references to colour in this figure legend, the reader is referred to the web version of this article.)

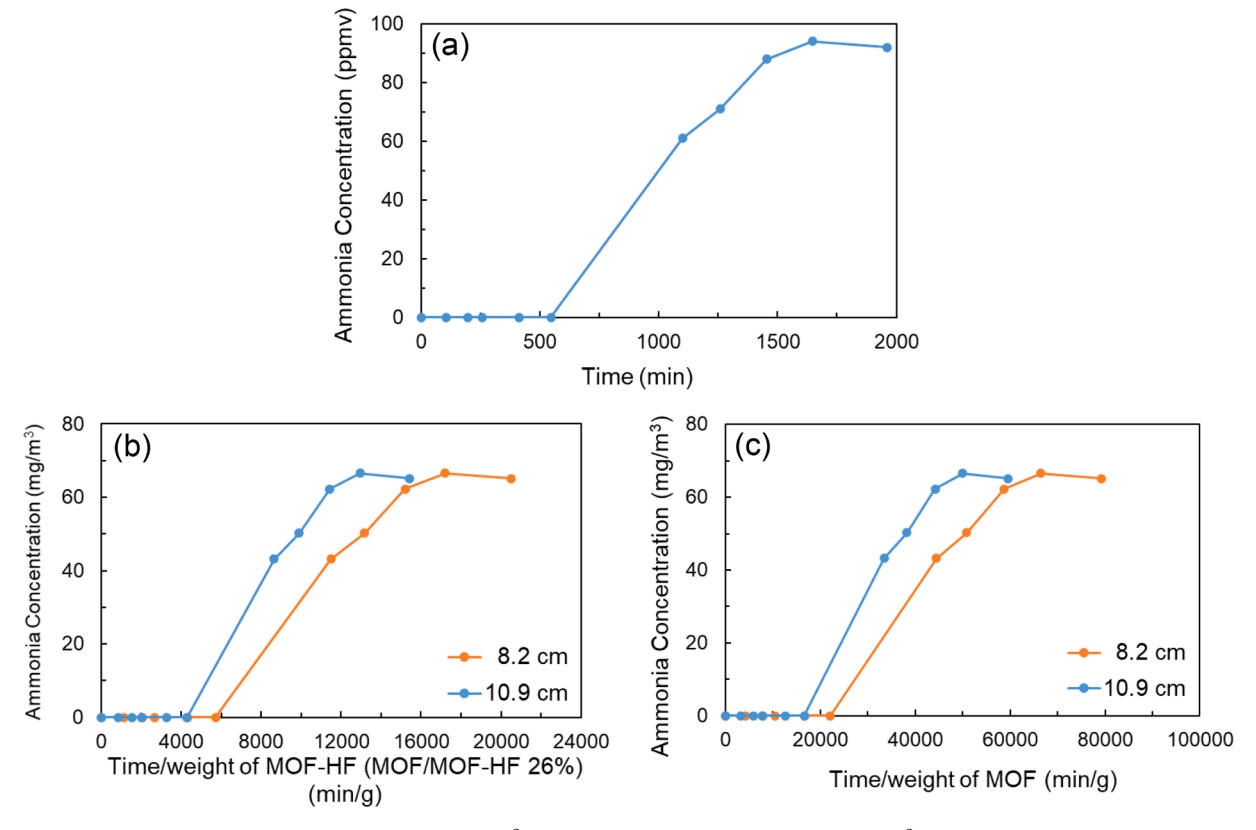


Fig. 7. (a) Ammonia breakthrough data with 100 ppmv (70.8 mg/m 3) NH₃-containing gas stream flowing at 10 cm 3 /min at a RH \sim 50 % through regenerated MOF-loaded Nylon HFM module (MOF loaded in HFM pores only); (b) normalized by weight of MOF-HFMs, and (c) normalized by weight of MOF. Blue lines plot the data calculated based on total length (10.9 cm) of the HFMs and orange lines plot the data based on active length (8.2 cm) of the HFMs. (For interpretation of the references to colour in this figure legend, the reader is referred to the web version of this article.)

of a HFM module (5 HFMs in the module; total outer membrane surface area of 12.88 cm² (Table 2 for module details)). The permeated gas was collected coming through the open tube side of the HFMs through the tube-sheet (Fig. 1 for HFM module and flow schematic; Fig. 2 for a photo of the module). (Open area of the flat MOF-filled ePTFE membrane film surface area [28] was smaller at 2.84 cm²). Fig. 6a results are illustrated in Fig. 6b via ammonia breakthrough behavior plotted against the x-axis describing the time/adsorbent weight where the weight includes MOF adsorbent plus HFMs. These results show that the breakthrough time is 50–100 % larger than that in an earlier work with flat membranes [28]: 3000–4000 min/g vs 2000 min/g. We see similarly the value to be around 2100 min/g for the MOF MIL-100(Fe) [22].

A more useful estimate would eliminate the weight of the HFMs which results in a high value of 12,000 to 15000 min/g of MOF as shown in Fig. 6c depending on whether we take the whole length of the HFMs or the active length of the HFMs since the section of the hollow fiber membranes potted in the epoxy tube-sheets near the gas entrance to the module is ineffective. In longer modules, the effect of the inactive length is reduced. Regeneration of this thin packed bed of nanocrystals of MOFs was implemented.

Fig. 7 shows the performance of the regenerated bed. The performance is somewhat better than the first sorption run (Fig. 6) indicating that solvent removal from the bed was incomplete before conducting runs with the virgin adsorbent. The performance of the bed after second regeneration is shown in Fig. 8. The performances appear to be similar to what we observe in Fig. 7.

It is useful to develop an estimate of the sorption capacity of nanocrystals of UiO-66-NH $_2$ MOF located in the submicrometer pores of the HFM for NH $_3$. Using a conventional packed bed of MOF particles in a 4 mm ID glass fritted tube, Jasuja et al. [17] report their NH $_3$ sorption capacity as 3.56 and 3.01 mmol/g for dry and wet gases respectively for

feed concentration levels of 1000 or 2000 mg/m³. We have calculated the ammonia sorption here by integrating the breakthrough curve for UiO-66-NH $_2$ MOF-loaded Nylon HFM-based module shown appropriately in Fig. S5 and the associated writeup including Table S1. It appears that the capacity up to the point when ammonia first appears in the outlet at a very low concentration is 0.86 mmol/g for the feed gas having 50%RH. When the complete feed breakthrough concentration is considered, the corresponding sorption capacity is 1.58 mmol/g. We could have substantially increased it by carrying out the solvothermal synthesis two more times [28,29]. The values obtained in the current study are still considerable considering our low feed ammonia concentration. Here the pore length /wall thickness of the MOF-HFM is only 200 μ m, which is 20 times less than the packing thickness (4 mm) used in the ammonia breakthrough testing made by Jasuja et al. [17].

We now focus on Nylon HFM module where the HFM bore had some microcrystals. The results are shown in Fig. 9 (a), 9(b), and 9(c). Fig. 9 (a) shows that the time when NH₃ first appears at trace levels in the outlet gas stream has been extended to 855 min. This is expected since larger adsorbent amount provides a higher sorption capacity and longer time for initial appearance. On the other hand, when we plot it in terms of breakthrough time/weight of adsorbent (w/without HFM), the times are longer indicating that sorption capacity of additional sorbent microparticles in the HFM bore are somewhat higher than that of the nanocrystals in the HFM pores only. (It suggests significant open space in the membrane pores (Fig. 4)). Thus, the MOF microcrystals located in the HF bores extend the contact time of ammonia molecules and MOF particles.

From the orange line in Fig. 9(c), we calculate sorption capacity to be 1.38 mmol/g (conditions for this calculation are similar to those of MOFs in membrane pores only). One reason for this result is that the NH_3 concentration in the gas was used in the testing was low (compared to a

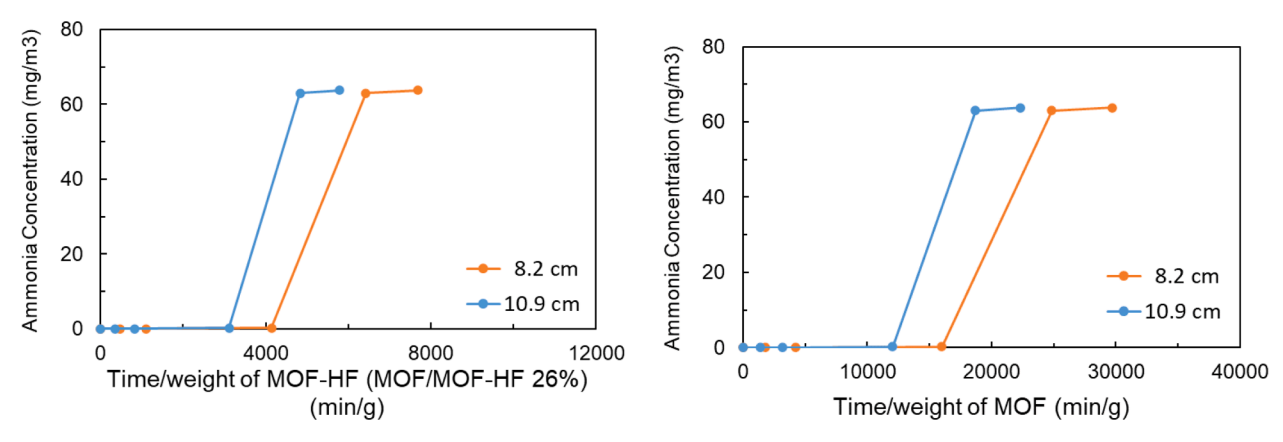


Fig. 8. Ammonia breakthrough testing with the 2nd time regenerated MOF-HFs with MOF crystals only existing in the HFM pores. (The MOF-HFs module was kept in the vacuum drying box at 60 °C for 3 days, then the regenerated module was kept in the desiccator without vacuum.).

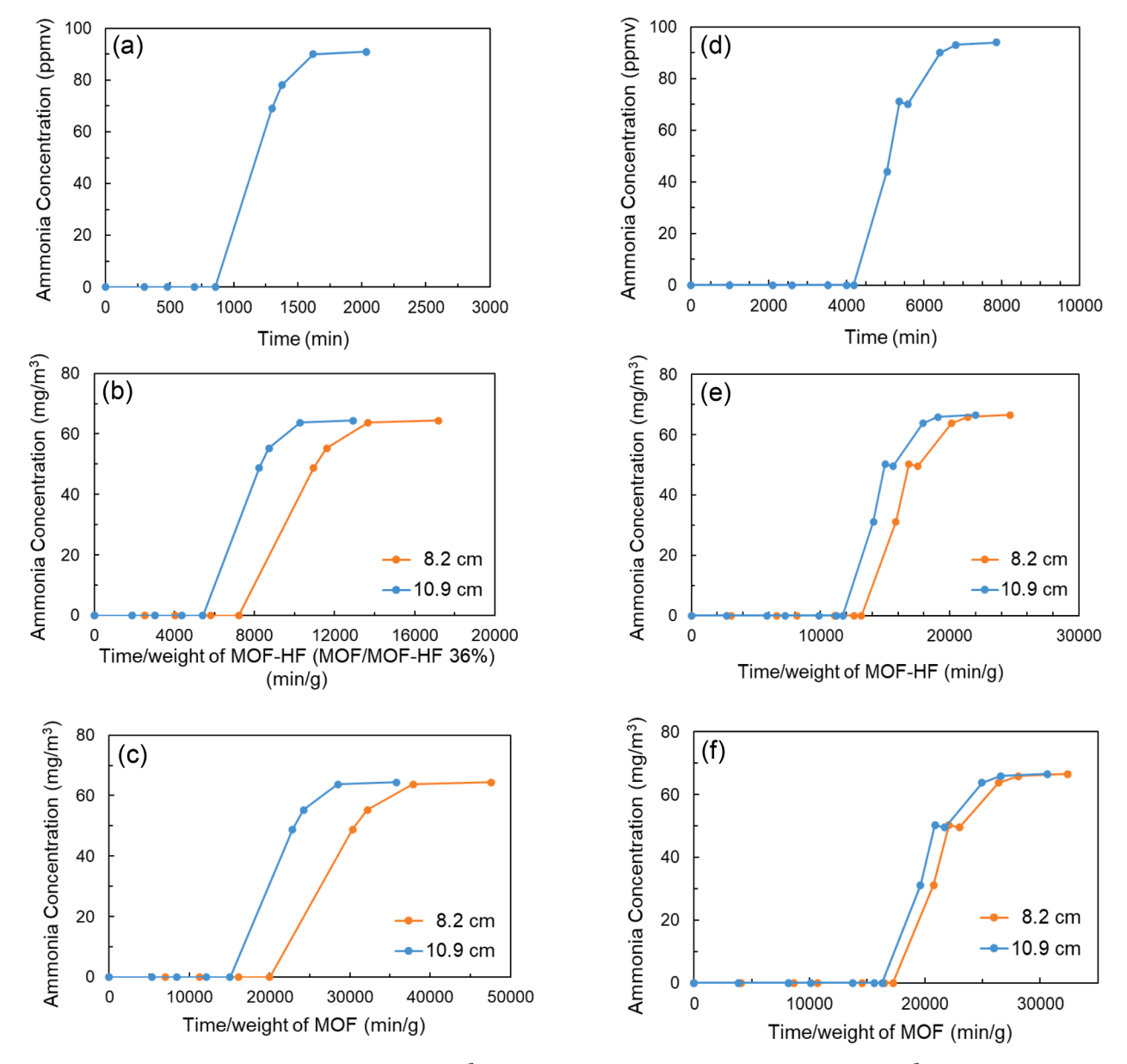


Fig. 9. (a) Ammonia breakthrough test with 100 ppmv (70.8 mg/m 3) NH₃-containing gas stream (RH \sim 50 %) flowing at 10 cm 3 /min through MOF-loaded Nylon HFM-based module, with MOFs in HFM pores and bores; (b) data replotted against time/weight of MOF crystals plus HFM; (c) data replotted against time/weight of MOF crystals only; (d-f) results of NH₃ breakthrough test under the same conditions for MOF-loaded Nylon HFM-based module, with MOFs in HFM pores, HFM bores and the extra capillary space. Blue lines plot the data calculated based on the whole length (10.9 cm) of the HFMs and orange lines are based on the active length (8.2 cm) of the HFMs. (For interpretation of the references to colour in this figure legend, the reader is referred to the web version of this article.)

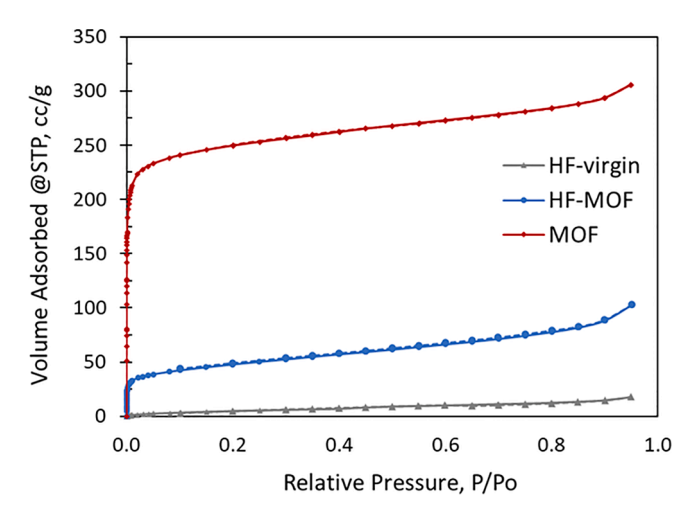


Fig. 10. N_2 isotherm plots at 77 K for virgin Nylon 6 hollow fiber membrane, Nylon 6 hollow fiber membrane with UiO-66-NH $_2$ MOF loading, and UiO-66-NH $_2$ MOF achieved during HF-MOF preparation. Solid lines represent adsorption phase and dashed lines represent desorption phase.

Table 3BET based surface area estimates.

Samples	Surface area (m ² /g)
Virgin Nylon 6 hollow fiber membrane	10
Nylon 6 hollow fiber membrane with UiO-66-NH ₂ MOF growth (weight percent of MOF: 26 %).	158
UiO-66-NH ₂ MOF achieved during HF-MOF preparation	983

much higher value of ~ 1000 ppm ammonia in other studies). An additional reason for this behavior is that HFM bores were not well packed with MOF microcrystals; no attempt was made to enhance the packing density since the goal was to demonstrate the concept and feasibility. But MOF loading in HFM bores increased the contact time of NH $_3$ to the adsorbent, UiO-66-NH $_2$ MOF.

Fig. 9(d), 9(e) and 9(f) illustrate the adsorption behavior when MOFs are located in HFM pores, the HFM bores as well as in the extra capillary space. Fig. 9(d) shows the overall adsorption behavior in terms of outlet

 NH_3 concentration vs time with trace level NH_3 showing up at ~ 4000 min. Fig. 9(e) and 9(f) show respectively adsorption behavior as outlet NH_3 concentration vs time/weight of MOF crystals plus HFM and time/weight of MOF crystals only based on the whole length and active length of HFMs. Between Fig. 9(c) and 9(f), the time/weight of MOF is approaching a high value of 20000 min/g of MOF.

3.3. BET and PXRD results

The N_2 adsorption and desorption isotherms are reported in Fig. 10 for virgin Nylon 6 HFM, Nylon 6 HFM with UiO-66-NH₂ MOF loading, and UiO-66-NH₂ MOF achieved during HF-MOF preparation. The y-axis unit of cm³/g refers to per gram of sample. The very sharp rise in the adsorbed volume in the plot at very low P/P₀ represents the narrow micropores (< \sim 1 nm) grown without membrane. Using Density Functional Theory (DFT) characterization methods, the pore size distributions determined from N_2 isotherms are shown in Fig. S6. The void size diameter for most of the synthesized MOF is 0.6 nm, which is consistent with the dimension of UiO-66 MOF reported by Cavka et al. [31]. The approximately sharp turn and subsequent slow increase implies narrow mesopores (<~2.5 nm) and macropores. Table 3 lists the corresponding BET surface areas. Pore size distributions were determined from N_2 isotherms by BET multiple-point analysis.

Fig. 11 provides the PXRD patterns of the virgin Nylon 6 hollow fiber membrane (HF-Virgin), UiO-66-NH $_2$ MOF synthesized in Nylon 6 hollow fiber membrane (HF-MOF), and UiO-66-NH $_2$ MOF (MOF) achieved during synthesis. PXRD patterns of the sodium dodecyl sulfate (SDS) are also included. These results demonstrate that the PXRD patterns of UiO-66-NH $_2$ MOFs synthesized are identical to the known PXRD patterns for this MOF; the two highest diffraction peaks at $2\theta=7.3^{\circ}$ and 8.5° correspond to its d-spacing of 12.1 Å and 10.5 Å. The PXRD patterns of HF-MOF contain the prominent peaks of MOF and HF-virgin; the main peaks of reactants ZrCl $_4$, H $_2$ BDC-NH $_2$ and SDS are not shown since these are identical to those reported earlier [28].

3.4. Tensile strength of Nylon hollow fiber membranes

The tensile strengths of virgin Nylon hollow fiber membranes and the Nylon hollow fiber membranes which underwent the MOF synthesis in its pores and outside at 120 $^{\circ}\text{C}$ for 18 h were measured. The results are shown in Fig. 12. It shows that virgin Nylon hollow fiber is somewhat more elastic than the Nylon hollow fibers which underwent the chemical

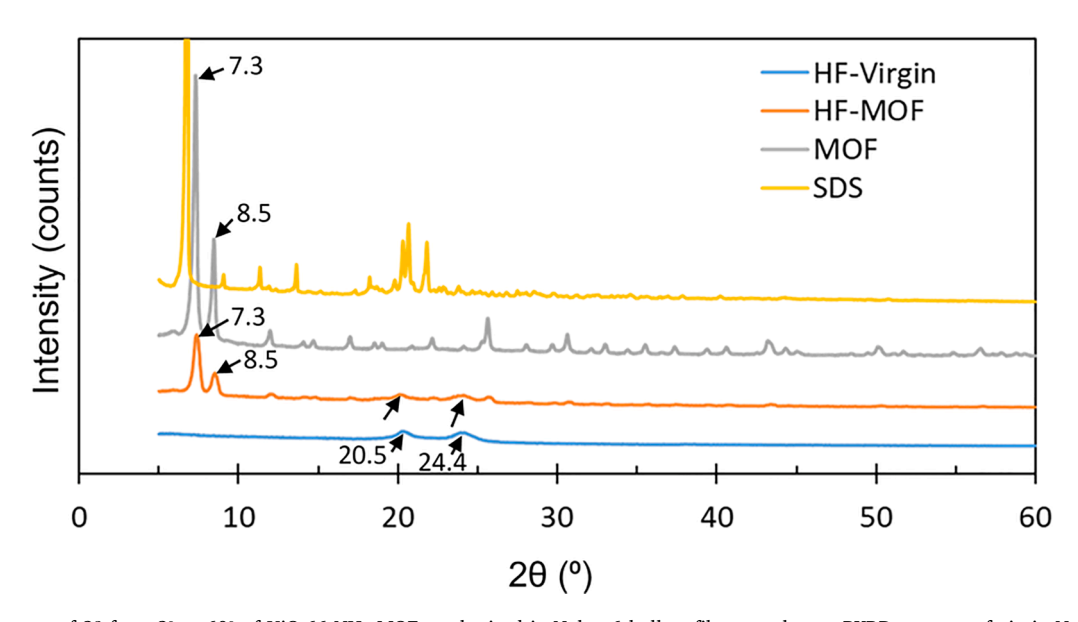


Fig. 11. PXRD patterns of 2θ from 2° to 60° of UiO-66-NH₂ MOF synthesized in Nylon 6 hollow fiber membrane; PXRD patterns of virgin Nylon 6 hollow fiber membrane, MOF achieved during synthesis and SDS are also shown.

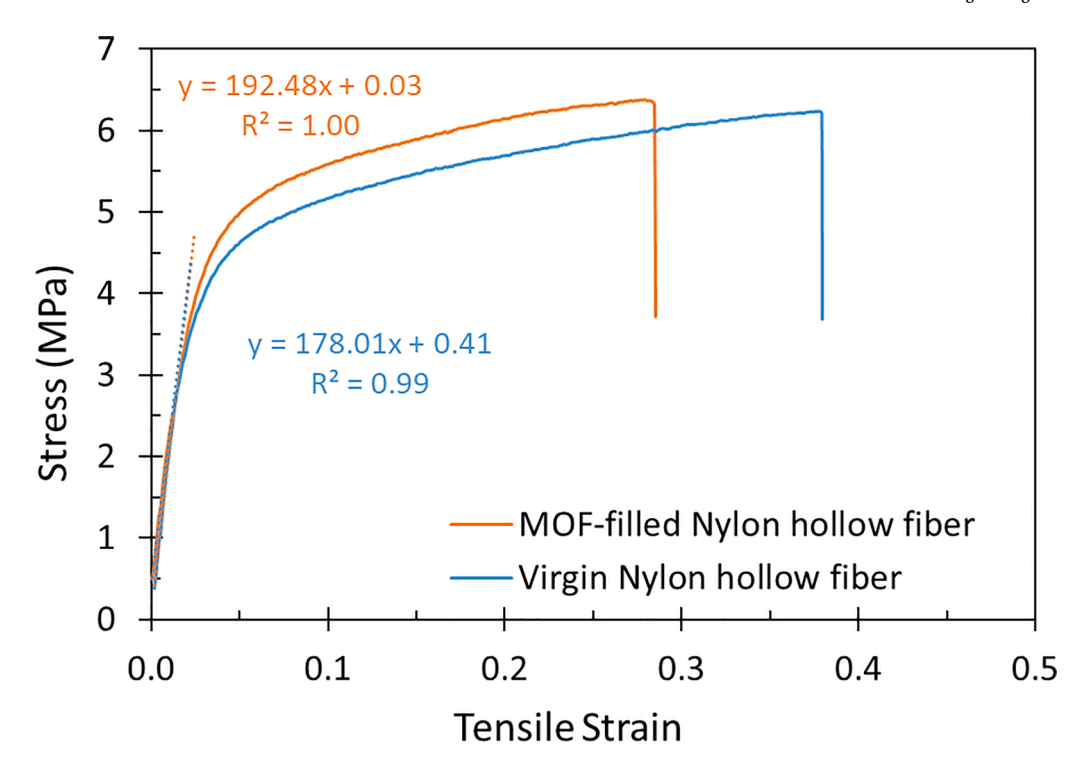


Fig. 12. Stress-strain behavior of virgin Nylon hollow fiber membranes and those Nylon hollow fiber membranes subjected to the MOF synthesis and has MOFs in membrane pores.

and thermal treatment for MOF formation. Yet the treated Nylon hollow fibers have considerable strength considering the high porosity the porous membrane structure has. From the slope of the stress/strain curve, the values of Young's modulus found were as follows: virgin Nylon hollow fiber is 178 MPa; MOF-filled Nylon hollow fiber is 192 MPa.

3.5. Further considerations on the technique

Direct utilization of the extraordinary sorption capabilities of microcrystals and nanocrystals of the UiO-66-NH $_2$ MOF in a high surface area adsorber has been achieved by solvothermal synthesis of the MOFs inside and outside the pores of porous hydrophilic Nylon HFMs packed in a cylindrical module. No special steps were needed here unlike other studies [28,29] since the organic synthesis solution for the MOF spontaneously wetted the pores of Nylon HFMs. This technique may be adopted for any kind of MOF synthesis as long as the HFMs are chemically and thermally compatible with the MOF synthesis environment. In addition, the issue of pore wetting by the synthesis liquid mixture needs to be considered as well. If the pores do not get spontaneously wetted, then pressure induced pore wetting may be implemented. For such cases, it would be desirable to carry out the synthesis using a potted HFM module so that pore wetting pressure can be applied.

We have essentially bypassed the need for processing MOFs obtained as loose powders into various shapes, e.g., granules, pellets, etc. by synthesizing MOFs in situ [25] with hollow fiber membranes. Further, the loss of the BET surface area due to processing loose MOF powders into various shapes via densification [23,26] is avoided. Here, we have the alternate arrangement of synthesizing MOFs in situ and then the device is ready to go after MOF synthesis. The issue of mechanical strength does not arise for crystals in the pores of the hollow fiber membrane. Microcrystals in the bore of the hollow fibers or in the extra capillary space do not have any demanding strength requirement: gas passes by such structures as the adsorption process-based exchange of molecules in gas phase goes on.

If two different MOFs are needed for efficient adsorption of two

different gases/vapors, such hollow fiber modules may be used [32]. However, the MOF incorporation methods will need to be changed. For example, one MOF may be incorporated in the pores via synthesis. Then the extra capillary space and the HFM bores may be washed free of the synthesized MOF and then a suspension of MOF nanocrystals and microcrystals of the second MOF may be brought in from the shell side and tube-side and the particular MOF incorporated there by removing the solvent/carrier liquid via filtration by blocking the module exits for the MOF particles (as shown in Fig. S1). One can extend it to three different MOFs by independently using the extra-capillary space for a second MOF and the hollow fiber membrane bore for a third MOF [29]. Further, if regeneration of each MOF may be carried out at a different temperature, one can have three packed beds in the same device each regenerated at a different temperature with shell-side feed of the gas and the product stream withdrawn through the tube-side or vice versa.

4. Conclusions

In conclusion, we have proposed and illustrated a convenient method for utilizing fragile MOF nanoparticles and microparticles in a compact HFM device for adsorption of gases/vapors via for example in situ MOF synthesis. HFM devices are modular and compact and are used in large scale for industrial membrane gas separations. Excellent adsorption performances were demonstrated by adsorbing ammonia from a dilute ammonia-containing gas stream in three configurations: MOF nanocrystals in the HFM pores; MOF microcrystals are present in addition in the HFM bore; MOF microcrystals are also present in the shell side of the hollow fibers, the extra capillary space. Nylon HFMs provide a convenient platform for direct synthesis of MOFs from a demanding solventbased chemical as well as thermal environment. This eliminates the need for making beads and pellets of MOFs and utilizes the high surface area per unit device volume provided by hollow fiber membrane as support. Although we have shown here results of adsorption of NH₃ from a gas phase, sorption of suitable adsorbates from a liquid phase has also been carried out successfully in such porous membranes filled with UiO-66-NH₂ MOF nanoparticles and microparticles.

Declaration of Competing Interest

A patent application filing is being undertaken.

Data availability

Data will be made available on request.

Acknowledgements

The authors gratefully acknowledge support for this research from DTRA contract # HDTRA 1-16-1-0028. This research was carried out in the NSF Industry/University Cooperative Research Center for Membrane Science, Engineering and Technology that has been supported via two NSF Awards IIP1034710 and IIP-1822130. We are grateful to W.L. Gore Inc. for donating GMM-404 membranes of ePTFE to our research. Dr. Michael Jaffe's Laboratory helped us with tensile strength measurements.

Appendix A. Supplementary data

Supplementary data to this article can be found online at https://doi.org/10.1016/j.cej.2022.140228.

References

- [1] X. Lu, X. Wang, F. Kapteijin, Water and metal—organic frameworks: From interaction toward utilization, Chem. Rev. 120 (2020) 8303–8377.
- [2] Q. Qian, P.A. Asinger, M.J. Lee, G. Han, R.K. Mizrahi, S. Lin, F.M. Benedetti, A. X. Wu, W.S. Chi, Z.P. Smith, MOF-based membranes for gas separations, Chem. Rev. 120 (16) (2020) 8161–8266.
- [3] X. Li, Y. Liu, J. Wang, J. Gascon, J. Li, B. Van der Bruggen, Metal-organic frameworks based membranes for liquid separation, Chem. Soc. Rev. 46 (2017) 2324, 2444.
- [4] J. Li, X. Wang, G. Zhao, C. Chen, Z. Chai, A. Alsaedi, T. Hayat, X. Wang, Metal-organic framework-based materials: superior adsorbents for the capture of toxic and radioactive metal ions, Chem. Soc. Rev. (2018), https://doi.org/ 10.1039/c7cs00543a.
- [5] L. Chen, Q. Xu, Metal-organic framework composites for catalysis, Matter. 1(2019) 57–89, July 10.
- [6] Y.S. Lin, Metal organic framework membranes for separation applications, Curr. Opin. Chem. Eng. 8 (2015) 21–28.
- [7] S. Sorribas, P. Gorgojo, C. Téllez, J. Coronas, A.G. Livingston, High flux thin film nanocomposite membranes based on metal-organic frameworks for organic solvent nanofiltration, J. Am. Chem. Soc. 135 (40) (2013) 15201–15208.
- [8] M. Kadhom, W. Hu, B. Deng, Thin film nanocomposite membrane filled with metalorganic frameworks UiO-66 and MIL-125 nanoparticles for water desalination, Membranes. 7 (2) (2017) 31.
- [9] Z. Zhao, X. Ma, A. Kasik, Z. Li, Y.S. Lin, Gas separation properties of metal organic framework (MOF-5) membranes, Ind. Eng. Chem. Res. 52 (3) (2012) 1102–1108.
- [10] J.Y. Lin, Molecular sieves for gas separation, Science 353 (6295) (2016) 121–122.
- [11] K. Eum, C. Ma, A. Rownaghi, C.W. Jones, S. Nair, ZIF-8 Membranes via interfacial microfluidic processing in polymeric hollow fibers: Efficient propylene separation at elevated pressures, ACS Appl. Mater. Interfaces 8 (38) (2016) 25337–25342.
- [12] J. Hou, X. Hong, S. Zhou, Y. Wei, H. Wang, Solvent-free route for metal-organic framework membranes growth aiming for efficient gas separation, AIChE J. 65 (2) (2019) 712–722.

- [13] G.W. Peterson, M.A. Browe, E.M. Durke, T.H. Epps III, Flexible SIS/HKUST-1 mixed matrix composites as protective barriers against chemical warfare agent simulants, ACS Appl. Mater. Interfaces 10 (2018) 43080–43087.
- [14] Q. Qian, A.M. Wright, H. Lee, M. Dincă, Z.P. Smith, Low-temperature H₂S/CO₂/ CH₄ separation in mixed-matrix membranes containing MFU-4, Chem. Mater. 33 (17) (2021) 6825–6831.
- [15] Approval of Respiratory Protective Devices. Code of Federal Regulations, Part 84, Title 42, (1995).
- [16] G.W. Peterson, J.B. DeCoste, F. Fatollahi-Fard, D.K. Britt, Engineering UiO-66-NH₂ for toxic gas removal, Ind. Eng. Chem. Res. 53 (2) (2014) 701–707.
- [17] H. Jasuja, G.W. Peterson, J.B. Decoste, M.A. Browe, K.S. Walton, Evaluation of MOFs for air purification and air quality control applications: Ammonia removal from air, Chem. Eng. Sci. 124 (2015) 118–124.
- [18] T.G. Glover, G.W. Peterson, B.J. Schindler, D. Britt, O. Yaghi, MOF-74 building unit has a direct impact on toxic gas adsorption, Chem. Eng. Sci. 66 (2) (2011) 163–170.
- [19] J. Zhao, M.D. Losego, P.C. Lemaire, P.S. Williams, B. Gong, S.E. Atanasov, T. M. Blevins, C.J. Oldham, H.J. Walls, S.D. Shepherd, M.A. Browe, G.W. Peterson, G. N. Parsons, Highly adsorptive, MOF-functionalized nonwoven fiber mats for hazardous gas capture enabled by atomic layer deposition, Adv. Mater. Interfaces 1400040 (2014), https://doi.org/10.1002/admi.201400040.
- [20] P.C. Lemaire, J. Zhao, P.S. Williams, H.J. Walls, S.D. Shepherd, M.D. Losego, G. W. Peterson, G.N. Parsons, Copper benzenetricarboxylate metal—organic framework nucleation mechanisms on metal oxide powders and thin films formed by atomic layer deposition, ACS Appl. Mater. Interfaces 8 (2016) 9514–9522.
- [21] M.S. Denny Jr, M. Kalaj, K.C. Bentz, S.M. Cohen, Multicomponent metal-organic framework membranes for advanced functional composites, Chem. Sci. 9 (2018) 8842
- [22] A.H. Valekar, K.-H. Cho, U.-H. Lee, J.S. Lee, J.W. Yoon, Y.K. Hwang, S.G. Lee, S. J. Cho, J.-S. Chang, Shaping of porous metal–organic framework granules using mesoporous ρ-alumina as a binder, RSC Adv. 7 (2017) 55767.
- [23] Y. Khabzina, J. Dhainaut, M. Ahlhelm, H.-J. Richter, H. Reinsch, N. Stock, D. Farrusseng, Synthesis and shaping scale-up study of functionalized UiO-66 MOF for ammonia air purification filters, Ind. Eng. Chem. Res. 57 (2018) 8200–8208.
- [24] M.I. Hossain, A. Udoh, B.E. Grabicka, K.S. Walton, S.M.C. Ritchie, T.G. Glover, Membrane-coated UiO-66 MOF adsorbents, Ind. Eng. Chem. Res. 58 (2019) 1352–1362.
- [25] M. Younas, M. Rezakazemi, M. Daud, M.B. Wazir, S. Ahmad, N. Ullah, S. R. Inamuddin, Recent progress and remaining challenges in post-combustion CO2 capture using metal-organic frameworks (MOFs), Prog. Energy Combust. Sci. 80 (2020), 100849.
- [26] M.I. Nandasiri, S.R. Jambovane, B.P. McGrail, H.T. Schaef, S.K. Nune (2016) Adsorption, separation, and catalytic properties of densifed metal–organic frameworks, Coord. Chem. Rev. 311, 38–52 (2016).
- [27] B.B. Shah, T. Kundu, D. Zhao, Mechanical properties of shaped metal-organic frameworks, Top. Curr. Chem. 377 (2019) 25.
- [28] Y. Song, J. Chai, K.K. Sirkar, G.W. Peterson, U. Beuscher, Membrane-supported metal organic framework based nanopacked bed for protection against toxic vapors, Sep. Purif. Technol. 251 (2020), 117406.
- [29] Y. Song, C. Peng, Z. Iqbal, K.K. Sirkar, G.W. Peterson, J.J. Mahle, J.H. Buchanan, Graphene oxide and metal organic framework based breathable barrier membrane for toxic vapors, ACS Appl. Mater. Interfaces 14 (2022) 31321–31331.
- [30] H. Wang, S. Zhao, Y. Liu, R. Yao, X. Wang, Y. Cao, D. Ma, M. Zou, A. Cao, X. Feng, B. Wang, Membrane adsorbers with ultrahigh metal-organic framework loading for high flux separations, Nat. Commun. 10 (2019) 4204.
- [31] J.H. Cavka, J. Søren, O. Unni, G. Nathalie, L. Carlo, B. Silvia, P.L. Karl, A new zirconium inorganic building brick forming metal organic frameworks with exceptional stability, J. Am. Chem. Soc. 130 (42) (2008) 13850–13851.
- [32] Q. Wang, J. Hu, L. Yang, Z. Zhang, T. Ke, X. Cui, H. Xing, One-step removal of alkynes and propadiene from cracking gases using a multi-functional molecular separator, Nat. Commun. 13 (2022) 2955.